The big puzzle: a critical review of virtual re-association methods for fragmented human remains in a DVI context'

Lise MALFROY CAMINE, Vincent VARLET, Lorenzo CAMPANA, Silke GRABHERR, Negahnaz MOGHADDAM

PII: S0379-0738(21)00353-4

DOI: https://doi.org/10.1016/j.forsciint.2021.111033

Reference: FSI111033

To appear in: *Forensic Science International*

Received date: 10 March 2021
Revised date: 26 September 2021
Accepted date: 27 September 2021

Please cite this article as: Lise MALFROY CAMINE, Vincent VARLET, Lorenzo CAMPANA, Silke GRABHERR and Negahnaz MOGHADDAM, The big puzzle: a critical review of virtual re-association methods for fragmented human remains in a DVI context', *Forensic Science International,* (2021) doi:https://doi.org/10.1016/j.forsciint.2021.111033

The big puzzle: a critical review of virtual re-association methods for fragmented human remains in a DVI context'

Lise MALFROY CAMINE[1,4], Vincent VARLET[1,4], Lorenzo CAMPANA[2,4], Silke GRABHERR[1,2,3,4], Negahnaz MOGHADDAM[1,2,4]

1. Swiss Human Institute of Forensic Taphonomy, University Centre of Legal Medicine Lausanne Geneva.
2. Forensic Imaging and Anthropology Unit, University Centre of Legal Medicine Lausanne Geneva.
3. Geneva University Hospital and University of Geneva. Geneva, Switzerland
4. Lausanne University Hospital and University of Lausanne. Lausanne, Switzerland

Corresponding author:

MALFROY CAMINE Lise

lise.malfroy-camine@chuv.ch

Swiss Human Institute of Forensic Taphonomy,

University Centre of Legal Medicine Lausanne Geneva,

Ch. de la Vulliette 4

1000 Lausanne, Switzerland

ABSTRACT

During a Disaster Victims Identification (DVI) mission, international protocols rely on interdisciplinary work, especially between specialists from forensic imaging and anthropology. In case of air crashes or explosions, DVI units may face thousands of fragmented human remains (FHRs). The physical re-association of FHRs and the identification process is very complex and challenging, and relies upon expensive and destructive DNA analysis. A virtual re-association (VRA) of these fragments, using Multidetector Computed Tomography (MDCT), could be a helpful tool in forensic anthropology analysis, as it could assist in reducing the number of DNA samples. However, there is no standardized protocol for including such an approach into a DVI procedure.

The aim of this study was to summarize and analyze existing techniques through a systematic review and to develop a protocol for virtual re-association of FHRs, adapted to the DVI context.

A keyword-based literature search was conducted, focusing on the VRA methods using MDCT imaging and 3D surface scan methodology. Reviews and primary articles, published between 2005 and 2020 in the fields of forensic anthropology, paleoanthropology, archaeology, and fracture reduction surgery were sorted out. A total of 45 publications were selected and analyzed based on their content and relevance.

The results show that research on the re-association of FHRs increased significantly during the last five years. Seven steps regarding the MDCT-based method for the virtual re-association of FHRs could be identified: acquisition of 3D-images, segmentation of the MDCT-data, post-processing and surface generation, identification of intact and fracture surfaces, identification and registration of matching fragments, and validation of the re-association.

The literature is surprisingly sparse regarding the FHRs re-association as a forensic tool, and mainly consists in case reports, whereas validated methods were presented in archaeology and surgery publications. However, we were able to adapt the MDCT-based approach for the virtual re-association of the FHRs and propose an innovative protocol for DVI missions. This protocol includes the needed details, from the acquisition of MDCT imaging to the virtual re-association of 3D models and its validation. Each step has to be fully tested, adapted and validated in future studies.

Keywords: Forensic anthropology / computed tomography / Fragmented Human Remains / Re-association / 3D images

1. INTRODUCTION

Medical imaging technologies have revolutionized the fields of medical diagnosis, surgery, but also forensic pathology, anthropology and archaeology [1]–[4]. Particularly in forensics, they allow the observer to obtain a snapshot of a material (tissue, bone, etc.) that inevitably degrades over time. Thus, second expertise, but also evidence consistency, are guaranteed through these innovative technologies [5]–[8]. Many medical imaging techniques have been adapted to the forensic field. The Multidetector Computed Tomography (MDCT) uses a rotating X-ray source combined to several opposing detectors. to acquire the internal and external morphology of a body. The attenuation coefficient of each tissue is analyzed through specific algorithm to reconstruct sectional 2D images and combine them as a 3D volume.

Various technologies have also contributed to the development of imaging-based forensic anthropology, or “virtual anthropology” (VA). One example is the forensic 3D surface scanning (3DSS), which derived from the industrial field. It allows for the recording of the external morphology, and depending on the device used, the texture and color of bones [8], [9].

These imaging techniques have increasingly been used over the past decade [9]–[12]. Currently, several forensic institutes have access to a MDCT unit, either using hospital equipment, or, more rarely, their own MDCT-scanner. [13], [14]. In Switzerland, every 7 forensic institutes can access at least external MDCT-scans, and the four academic have an in-house device.

MDCT and 3DSS methods have been used for the determination of biological profile, the identification of bone pathologies, recent or healed traumas, and the detection of prosthetic materials (orthopedic, cardiovascular, and so on)[5], [7], [8], [11]. This data helps to reduce the number of potential matches for the identification process, and leads to a comparative identification through e.g. odontology, frontal sinuses comparison, or implants labeling [15], [16].

The application of VA is therefore fundamental for situations when a high number of bodies are to be identified, i.e. Disaster Victim Identification (DVI) missions. These are set up in case of mass disaster, or the analysis of mass graves. Prior to any medicolegal examination, a MDCT-scan is recommended by international DVI guidelines [17], [18].

Especially, in case of explosions, fire accidents, or aircrashes, the remains are fragmented or altered. Forensic anthropology and imaging may be highly relevant for the analyses**.** E.g., the 2001 tragic terrorist attack of the World Trade Center is one of the most complex DVI missions, due to the high number of victims (2 749) and to the heavy fragmentation degree and commingling (over 20 000 FHRs recovered). Forensic anthropologists were highly involved from recovery and triage to the identification process. These anthropological analyses of the FHRs traditionally requires extensive handling [19], and sometimes a maceration and cleaning process that can compromise DNA analysis [20]. In contrast, the use of MDCT-scans allows a direct access to the bone structure with minimum handling [7], [19], [21], [22]. The acquired data represents negligible physical space for storage and are easily transferred [23]–[25].

Moreover, the physical re-association of complementary fragments is an indispensable process for the identification, by reducing the number of samples to be taken for DNA analyses [19], [22], [26]–[28]. However, physical reconstruction may be very time-consuming, and may postpone subsequent analyses for comparative identification purposes. It relies on reconstructive adhesive materials such as glue, tape, or wax that can alter the bone tissue, are difficult to remove, and as such compromise later reconstruction [22].

The digital reconstruction of the FHRs along with physical examination, however, could reduce potential damage to the fragments. MDCT being currently included in the DVI process [17], [29], [30], a virtual re-association (VRA) of digital FHRs would be of great help if implemented before the classical identification protocol. It may also present some limitations, especially regarding the difficulty to segment and reconstruct very small fragments and burnt remains.

This article is a synthesis of existing methods for 3D documentation of fragmented bones, VRA and reconstruction of FHRs, from the fields of archaeology, orthopedic surgery, and forensic anthropology. The aim of this research was to summarize existing techniques through a systematic review and eventually to develop an appropriate protocol for the virtual re-association of FHRs that is reliable, quick, and that can easily be applied in a DVI situation.

2. METHODS

Literature search of PubMed, Web of Science and Science Direct was conducted for the 2005 to 2020 period, using three sets of keywords: “fragments/ fragmentation/bone fracture”, “3D/virtual”, “re-association/reassociation/reconstruction/reduction”, investigated in specific fields: archaeology, forensic anthropology, forensic odontology, orthopedic surgery, engineering and morphometric geometrics (Fig. 1 ; Tab.1).

Our review mainly focused on MDCT imaging for VRA of FHRs, though since surface scanning is widely used in archaeology and 3D engineering, the methods for re-associating fragments from surface scans were also considered.

Reviews and primary articles in English were selected and sorted out by relevance using the browser’s algorithm (automatic selection, based on the decreasing occurrence of the combined keywords). The 100 most relevant publications of each field (first articles sorted out by the algorithm) were considered, resulting in a list of 647 publications. Duplicates were deleted. Among the 224 remaining titles, 114 publications were excluded as they were mainly focused on methods for facial reconstruction, missing parts completion, distortion correction, surgical fixation, in situ surgical procedure, post-surgery healing, and 3D printing.

The remaining 110 publications were analyzed by title and abstract content, and 24 publications that correctly fitted with our subject (i.e. that specifically explained methods for fragments re-association) were reviewed. 15 additional articles, referenced in the selected publications, completed the list. From these 39 articles, 33 were primary [3], [4], [24], [25], [31]–[55], [22], [56], [57] and 6 were reviews [2], [7], [11], [14], [58]–[60].

It appeared that the segmentation step itself required a short review (Tab. 1). A preliminary research in the same databases with “segmentation” and “fragmented bone”/“fracture” keywords resulted in 6 additional publications [61]–[66].

In total, 45 articles were analyzed for this review, with the aim to define the state-of-the art of forensic anthropology methods for fragments re-association using MDCT-scan imaging.

3. RESULTS

During the past five years, the literature considering fragments re-association methods through imaging processes considerably increased (Fig. 2). Publications regarding surgical treatments have largely contributed to this specific field (Fig. 3).

From this review, most MDCT-based methods for fragments re-association describe seven necessary steps [32], [37], [48], [63]:

1) Acquisition of 3D -images
2) Segmentation of the MDCT-data in order to generate discrete closed surfaces
3) Post-processing and surface generation
4) Identification of intact surfaces and fracture surfaces (optional step, depending of the chosen re-association method)
5) Identification of matching fragments
6) Registration of matching fragments
7) Validation of the re-association

3.1. ACQUISITION OF MDCT-IMAGES

Our review shows that MDCT is an important tool for the virtual re-association of fragmented human remains (Fig. 4).

Many articles insist that the used acquisition parameters are a crucial factor for the quality of the reconstruction of the digital 3D-model. Published research by Grabherr et al. (2009) and Uldin (2016) have shown their importance for the accuracy of the measurements and anthropological observations on the obtained digital models [5], [7].

A total of 26 articles presented methods based on MDCT data [2]–[4], [7], [14], [25], [32]–[40], [43], [44], [46], [48]–[50], [52]–[54], [67]. Among them, 15 publications described, at least partially, their acquisition protocol [3], [7], [25], [32], [33], [35], [40]–[44], [48], [50], [52], [67], and only 3 provided their full protocol [7], [35], [44]. Based on the published data, the following range of parameters and device specifications is used for the MDCT acquisition and virtual reconstruction of non-fossilized skeletal remains:

- 64 detector rows [35], [61]
- Slice thickness: 0.2 mm [32], [55], 0.33 mm [25], 0.5 mm [32], 0.625 mm [40], [67], [67] 0.9 mm [35], 1.0 mm [39], [40], [44], [50], [62], [66], 1.4mm [62], 1.5 mm [3], [52], 2.0 mm [66]
- Spacing between overlapping slices: 0.3 mm to 0.5 mm [32], [35], [61], 0.625 mm [48], [48], 1.0mm [44]

Only one study conducted a review of acquisition parameters in a biological profile evaluation purpose, and proposed a full protocol [7], that fits within the range of published parameters and device specificities used for skeletal analysis and fragments reconstruction reviewed herein:

- 64 detector rows (as opposed to 8 detector rows)
- Voltage 100 kV
- Amperage 120mA
- Speed 1 sec/rotation
- Slice thickness 0.625 mm
- Spacing 0.3 or 0.6 m

By increasing the number of detector rows, and choosing thin slices and wider overlapping, the accuracy of the acquisition is enhanced. Such parameters, however, can also create imaging noise and, by increasing the weight of the data and the number of the slides, the reconstruction time may be considerably lengthened. The number of fragments to scan at once have to be taken into account in order to decrease the data weight.

Considering 3DSS, a total of 12 publications focused on it for VRA of fragments [14], [22], [24], [31], [33], [41], [45], [51], [55]–[57], [67]. Unlike the MDCT-scan that constitutes the first step of the DVI post-mortem examination, 3DSS is too time-consuming for a DVI context, and we did not investigate the parameters used for the acquisition with those scanners.

3.2. SEGMENTATION OF THE CT-DATA IN ORDER TO GENERATE DISCRETE CLOSED SURFACES

While the surface scan images are directly converted into surface format, MDCT-scan data have to be segmented, in order to obtain discrete surfaces from the radiography slices [2].

The first segmentation step is the individualization of each bone fragment from the CT-data if several fragments were scanned within one acquisition. The accuracy of the segmentation is a crucial factor for the success of the final 3D reconstruction [2], [31], [37], [63]. Indeed, over- or under segmentation may impede jigsaw-puzzle solutions, and the separation of fragments that share a contact (touching fragments) may represent a specific issue.

Different segmentation methods have been used in the literature (Fig. 5):

Manual segmentation

Manual segmentation only concerned 4 publications of our review. This process consists in a 2D, slice-by-slice, selection of bone fragments pixels [3], [4], [43], [50].

Automatic thresholding

Each tissue presents a specific attenuation of the incident X-ray, or radiodensity in Hounsfield Units (HU), that is specific to its composition and density, which is visually computed into pixels with a specific grey level. Using an automatic thresholding algorithm only discards pixels out of a defined interval of radiodensity (HU), thus segmenting only bone tissue [3].

While widely used - by 14 publications among 39 in our review (Tabl. 1) - simple automatic thresholding does not consider the variation of bone density (diaphysis to epiphysis, for example). Near the joints, cortical bone gets thinner and may even disappear. In this area, it can have an intensity similar to the surrounding soft tissues, resulting in an over or under-segmentation [63]. To solve this problem, Rathnayaka et al. (2011) proposes a multi-thresholding segmentation of the cortical bone, with thresholds adapted to anatomical regions [61]. According to its authors, this method allows for quick, accurate, and reproducible reconstructions, but it requires knowledge of which anatomical regions are analysed. Furthermore, this process cannot separate touching fragments. Multilevel thresholding method is used in 4 publications in our review, either as principal technique or as part of the segmentation protocol [46], [49], [52], [61].

Automatic region growing techniques (ARG)

ARG is applied in 5 publications of our review [4], [44], [50], [65], [66]. Also based on the CT-intensity mapping of each voxel, the algorithm considers contiguous pixels with a HU values in a defined CT-intensity interval as belonging to the same surface. This method is fully automated, and does not depend on the anatomical location of the fragment. However, for now, touching fragments cannot be automatically separated using ARG technique only.

Automatic placing seeds (APS) methods

All the segmentation methods mentioned above share the same limit in distinguishing touching fragments, especially for comminuted fractures. In addition, due to MDCT image resolution, close fragments can appear as joined and an operator-conducted post-segmentation step is therefore necessary to separate them. APS algorithms represent a solution for splitting these fragments. From 2011 to 2020, 7 publications of our review used APS methods for segmentation, all of them from the orthopedic surgery field [46], [48], [49], [52], [62]–[64].

Following Huang in 2011, Paulano proposed in 2014 an approach that, according to its authors, labels and separates fragments during segmentation [62], [63]. This method consists in manually placing a virtual seed in known distinct fragments, and applying simultaneous region growing algorithm. This algorithm considers homogeneous pixels -contiguous pixels with small differences in their intensity values (HU) - as belonging to a unique fragment. It therefore allows for splitting, and labeling fragments in contact with one another.

A following study from Nysjö [64] added a preliminary volume rendering technique to the placing seeds methods, so the operator can draw seeds directly on the surface of the 3D model.

More recently, an innovative method from Irwansyah [46], [49] combined in a single software (Physiguide®) a multi-level thresholding in order to automatically select seeds, and in a second step the placing seeds technique. This method has the advantage of being almost fully automated, and appears to successfully separate contiguous touching fragments while labeling them.

APS has been recently used for the segmentation of paranasal sinuses in a forensic identification objective [68].

3.3. POST-PROCESSING AND SURFACE GENERATION

In order to work on the 3D volume reconstructions from 2D images, the initial 2D Digital Imaging and Communication in Medicine (DICOM) files are converted into Surface Tessellation Language (STL, or Stereolithography) files [2], [14], [69].

The surfaces (triangular meshes or points clouds) may present errors, such as holes, pikes, or breaks. For a forensic purpose, and especially for geometric morphometry-based fragments re-association, the original surface should not be modified as corrections might alter the next steps of matching and registration. An extremely accurate data acquisition is preferable. However, in case of radiological artifacts, numerous 3D softwares offers options such to fix holes and remove breaks.

Specific softwares are commonly used for segmentation, 3D volume rendering and post-processing. It may be necessary to use complementary softwares for further surface modification, registration (3D superimposition of two surfaces based on their similarities by minimizing the distance between their points clouds) and comparison (Tab. 2).

3.4. IDENTIFICATION OF INTACT SURFACES AND FRACTURE SURFACES

The identification of fracture surfaces reduces the areas to compare. Thus, the calculation for automatic matching and registration is simplified. It is especially useful in cases of multi-fragmentation, meaning that each facet of a fragment can be complemented by several partial fractured surfaces. Our review exposes different methods for identifying the limits of fracture surfaces (Tab. 3):

CT-intensity based methods:

During the segmentation, semi-automatic methods from Willis (2007) and Zhou (2009) [32], [37] synthesize the CT-intensity (Hounsfield units) of each pixel as a histogram, that is splitted in two interfitting gaussian curves by the mixed gaussian method : the trabecular bone (TB) constitutes the curve of lower value and the cortical bone (CB) constitutes the higher intensities curve, and appropriate statistical thresholds are calculated for TB and CB. This method identifies the fractured surface as exposed TB, either by simple thresholding [32], [37] or through the placing seeds method [63].

Post-segmentation methods:

After the segmentation and reconstruction of the fragment surface, the identification of the fracture surface can be done by a visual evaluation of the 3D model [34], [36], [52]. Although quick, the reliability of the representation of the fracture outlines is uncertain.

Other automatic methods are based on roughness analysis, first points in contact methods, automatic outlining of the fracture through curvature analysis, etc.

In 2017, Mahfouz et al. presented a roughness-based technique for identifying fractured surfaces of fragmented crania, innominates, humeri and femurs. Roughness criteria is quantified by the amplitude of the deviation of the normal vectors at each point of a surface. It represents the variation in the height of micropeaks and valleys. The roughness of the external surface of an intact bone template was calculated and converted into a histogram with two components (gaussian curves): smooth and rough. When fractured, the roughness histogram presents a third high roughness component corresponding to the fracture surface. They showed that this method allows for isolating fractured surfaces that present roughness values similar to this third curve [67].

Considering that the fracture generates surface irregularities and exposes irregular trabecular bone, the fractured surfaces consists of the points with a high degree of roughness [31] or curvature [50]. While these methods are fully automated, according to the authors, some bones may present complex anatomical features that can be wrongly interpreted as fracture surfaces.

From a different point of view, Paulano-Godino and Jiménez-Delgado built a method considering that the fracture surface of a fragment consists in the “first points in contact” with the complementary surface [48]. This semi-automatic method manually sets fragments in a roughly appropriate relative position. Each fragment was contained in a virtual 3D frame, or bounding box. Both frames were displaced closer to each other following a virtual line between their respective centroids, until the two point clouds were in contact. The boxes were subdivided in 3D grids composed of voxels. The first voxels of each grid presenting at least one point from both surfaces were considered as belonging to a fracture surface. In this method, fracture surface edges depended of the considered pair of fragments. Consequently, each fragment was compared to every others to select the largest fracture (see section 5). This method quickly led to the final registration (see section 6). However, even if these steps were quickly achieved (less than 2 seconds by fracture surface merging) in case of high fragmentation degree, it would have to be repeated numerous times to obtain the matching corresponding surfaces, which might be too time-consuming.

3.5. IDENTIFICATION OF MATCHING FRAGMENTS

Several authors highlighted that a challenging aspect of fragments re-association in case of high fragmentation is the pairwise matching complexity [34], [48], [50]: one fragment has to be compared to multiple others, each of them presenting several fracture surfaces. This problem is frequently encountered by archaeologists when commingled ceramic fragments are to be reconstructed. According to a recent review of computer-aided methods for archaeological ceramics reconstruction [60], a two-step procedure is commonly used : first, a preliminary classification step that reduces the number of possible matches, then a local or global shape-based matching of the fracture surfaces can be applied. In surgery planning as for anthropological cases, same matching methods are used.

The identification of complementary fractured surfaces can be visually processed [4], [46], [49], [52]; nonetheless, in case of complex fragmentation, this combinatory problem of pairwise matching can require an automatic method. Orthopedic surgery frequently encounters this situation and different virtual methods have been built to allow rapid and reliable preoperative fracture reduction planning [2], [48](Tab. 4).

Operator-directed matching:

Twenty studies rely on an operator directed matching [3], [4], [22], [24], [25], [32], [33], [37]–[40], [42], [43], [49], [52]–[57]. This method relies on the operator’s knowledge in osteology and on the visual comparison of the fragments morphology. It is quick and simple for non-mixed fragmented bones from a single individual, though subjective.

Automatic pairwise matching:

Template-guided re-association methods are based on the matching of a fragment with the intact surface of an anatomical model, or template.

Anatomical landmarks can be used for locating a fragment onto an individual or statistical template (average bone morphology calculated from a sample of intact bones). This method requires previously identified fragments and sufficient landmarks on them, which may be lacking with small size fragments [39], [40], [54].

Another criterion for this template-guided re-association is the comparison of roughness and curvature features with intact templates. This method requires a pre-calculation of roughness or curvature values of a statistical template and the identification of anatomical features: different algorithms have been developed in digital engineering for archaeological purpose, such as Geodesic Disk spectrum and Heat Kernel signature [41]. Features mappings of the intact surface of the fragment are then compared to different bone type templates and placed onto the corresponding one [41], [45], [51], [67]. At this step, this method does not aim to fit a fragment with another, but rather to allocate each fragment to a probable position on the template, so that likely associations are quickly highlighted. The authors put forward the advantage of this method in case of missing fragments, when re-association can be done at least as an orientation tool for individualization. They nevertheless expose the main limit of this method, that requires previous statistical templates, therefore, an extended database of intact bone MDCT-scans. It is still unclear if the population and sex categorization of the template may have an impact on the efficiency of the method, nor if commingling situations can be solved without an operator-directed intervention.

Fragment-to-fragment re-association methods are based on the consistency between two fragments. They can consider the shape similarities of intact surfaces (surface extrapolation) or the complementarity of the fractured surfaces (roughness pattern, etc.).

The global shape of the fragment is a first criterion for fragment-to-fragment re-association [42], [44]. In one study published by Kikuchi and Ogihara [42], a morphometric geometrics algorithm calculates the global curvature of the fragment, and converts it into a Bezier curve (the mathematical transcription of a smooth curve, defined by the position of four or more control points in vector graphics). An intact surface extrapolation algorithm then predicts the curvature of the complementary fragments. Fragments with interpolating curves are considered as matching fragments and will be registered for a better fitting of their curves. The authors put forward the limitations of this technique: intact surface extrapolation seems appropriate for large fragments that can present Bezier curves specific enough to be compatible with few complementary fragments. It however requires an operator-induced matching in case of high fragmentation: For small fragments, this method may result in false positive matches, and more investigation is needed on the implementation of this methods for high fragmentation degrees.

The first points in contact method can be used for fragment-to-fragment re-association [37], [48] (see section 4). Both surfaces with the maximum number of voxels of contact are considered as best matches. As already mentioned, this method needs to test each fractured surface, with every other available surfaces and, according to its author, is limited by the number of fragments.

Winckelbach developed another method using surface-in-contact for pairwise matching [34]. For each point of the fracture surface the normale (the vector that is strictly perpendicular to the surface) was calculated, then aligned with corresponding normales of a possible matching surface. This represents the first registration step, which was then conducted for each complementary surface. The global surface-in-contact was calculated. By reducing the surfaces to smaller subsets, the optimal relative position of the fragments was iteratively calculated. According to the authors, this method requires 1 to 9 seconds for a surface comparison.

The last criterion for fragment-to-fragment pairwise matching of fractured surfaces is their local shape, through the surface roughness mapping. Huang considered the patterns of high roughness on the fragmented surface as feature clusters [31]. Patches of feature clusters are then targeted and multi-fragment automatic registrations are performed, based on these clusters as landmarks. Interpenetrating fragments are eliminated, and non-interpenetrating surfaces are considered as matching surfaces. This method quickly highlights mismatches, and anticipate the last step of fine registration of the fragments.

3.6. REGISTRATION OF MATCHING FRAGMENTS

Once the matching fragments have been selected, it is necessary to bring them together in order to minimize the space between their fractured surfaces, and to finally merge them into a restored piece (Tab. 5). As the surfaces are partially similar, the choice of the reference and moving models may influence the result [68]. The registration step can be manually done in a virtual environment, or by adjusting selected opposite landmarks, or features of the fracture surface, or by adjusting intact touching surfaces with each other or onto a statistical template. The final registration of different fragments can then be automatically performed with specific algorithms (mainly, iterative closest point, or ICP).

Operator-directed merging:

Operator-directed merging in a desktop environment [22], [24], [53] consists in the manual alignment of the fractured surfaces in a desktop environment and requires minimum material. As such, it can be easily employed in any situation, including DVI missions.

This method is directly derived from the physical reconstruction, and the previous choice of matching fragment is, classically, operator-directed. According to the referenced authors, the manual registration is more accurate and reliable than the physical reconstruction, mainly because of the lack of gravity and the possibility to carry out several tries before choosing the best alignment.

Virtual reality can be a complementary tool for operator-directed reconstruction [11], [25], [47]. Although the technology of VR headsets makes them more comfortable, high fragmentation cases would imply a long-lasting use that may visually and physically fatigue the operator. It is worth noting that haptic technology, which allows for a tactile response when “touching” a virtual object, seems to enhance the quality of the reconstruction, compared to manual or desktop reconstruction [33], [38].

Finally, thanks to the recent technological advances of 3D printers, fragment models can be physically replicated as shown by Collings et al. and Johnson et al, 2019 [55], [56]. They showed a manual merging of such replicate allowing the physical reconstruction of compromised fragments. However, in these studies the fragments were known to belong to one individual only.

Semi-automatic registration:

A virtual merging of the 3D reconstruction of the fragments can be performed with a minimal intervention of the operator by either using a global shape or a local shape of the fragments.

The global shape of the fragments was used by Kikuchi and Ogihara, who extended the surface extrapolation technique to set the complementary fragments in the appropriate relative position so that their Bezier curves fit at best [42].

The local shape has also been used, initially by Huang, 2006[31]. This work was then resumed by Yu 2012, Du 2016 and Yin 2018. Previous roughness analysis had highlighted feature clusters on the fracture surface, which were used to register complementary fragments [41], [45], [51].

These methods allowed a first rough registration that further needs to be refined. Automatic fine registration algorithms are frequently employed during a second stage [31], [32], [37], [45], [46], [51], [56], [67].

Automatic registration:

In 2017, Paulano et al performed fragments registration by using the first points in contact as landmarks. The relative position of each surface was then automatically refined [48].

The main algorithms used for fine registration of complementary surfaces are ICP (Iterative Closest Point) and LSTE (Least Square Transformation Error): these calculations get the surface in appropriate relative position so that the component points are globally as close as possible [2], [24], [37], [48], [67].This method can possibly be weighted by a CT intensity coefficient (based on Hounsfield unit) favoring the iterative registration of cortical bone points [32].

3.7. VALIDATION OF THE RE-ASSOCIATION

Once every matching fragment chosen and registered, the fragmented bone can be reconstructed. The efficiency of the reconstruction method is evaluated by comparison with an intact model, a template, or a physical reconstruction. Different criteria can be used. While a visual evaluation can be done, a quantitative method is more accurate and less subjective. Thus, mesh-to-mesh distance, landmarks superimposition or metric dimensions constitute better criteria.

Comparison with physical reconstruction (using wax, glue, etc.) is mostly employed in order to evaluate the expected advantages of a virtual reconstruction (enhancing of reproducibility and repeatability, speed, etc.) versus physical reconstruction, rather than evaluating the accuracy of the virtual reconstruction itself [24].

In order to assess the accuracy of the reconstruction and thus to validate the re-association method, the ideal process is to compare the reconstructed model with the model of the intact bone before its fragmentation [25].

However, in a real case scenario this so-called intact model is missing. Therefore, a statistical template, constructed from a CT database of intact bones, can be calculated as mentioned in the paper of Mahfouz [67]. This process requires a sufficient database of different bone types, if possible, scanned with the same method, parameters and devices. The average morphology is considered as a reliable template for comparisons, but the influence of sex and ancestry, however, remains unclear.

Without any previous intact model nor adequate available database, individual templates have been previously used [22], [35], [44], [57]. These studies compared the reconstruction to an intact model from an individual with a similar biological profile. This method requires rigorous evaluation of the biological profile, and is contested for individual identification purposes.

The consistency of the reconstruction and regularity of the merging surfaces can be roughly evaluated by visual means. Although this procedure is subjective, it can be a first step for a quick exclusion of false matches [31], [41], [50]. Printed 3D model re-association could be an additional method for an operator-directed physical fit analysis [55].

A more reliable criterion for validation is mesh-to-mesh comparison. Automatic algorithms such as TPS (Thin Plate Spline) or ICP (Iterative Closest Point) evaluate the distance from each point of the reference model (intact model at best) to the virtual reconstruction surface. The TPS algorithm places both surfaces in a position that minimizes the distance between them, then calculates the necessary energy for deforming the questioned surface so that it fits perfectly with the reference one, while the ICP algorithm calculate the point-to-point distance from a surface to the other. The result can be expressed as cumulative energy for TPS or mean/median distance for ICP. A colored map of the differences between the models can be edited, in order to show the location of inaccuracies or to illustrate the correct fitting of both surfaces [44].

4. **DISCUSSION**

Throughout this review, it appeared that the literature considering the virtual methods for FHRs re-association in forensics is surprisingly sparse, and mainly consists in case reports. Few studies proposed a validated protocol, testing the inter- and intra-operator variability [24], [25] or the rate of correct automatic matching [45].

In contrast, other fields such as archaeology and or surgery already explored the perspectives of computer-aided (human or non-human) re-association of fragments, and their advances could greatly benefit forensic anthropology.

This review summarizes the existing methods for FHRs re-association methods in forensics, anthropology, archaeology, orthopedic surgery, and within various engineering specialties, in order to highlight their respective advantages and drawbacks. The objective is to identify appropriate methods for a DVI situation when clear protocols have to be proposed to specialized units at an international level. MDCT imaging has proven to be a crucial tool in DVI missions [70] and its use for the virtual re-association of fragments would represent a valuable complement for enhancing the efficiency and quality of the remains identification.

Therefore, the re-association protocol has to be quick, easy-to-apply, and cost-efficient. Most important, it needs to yield reliable results in order to enhance the victim identification process.

Thanks to the careful review of the literature, an innovative protocol is proposed, which aims to optimize MDCT-scan parameters and segmentation steps, and to move forward towards a maximal automating of pairwise matching and registration in the future.

4.1. Acquisition of 3D –images:

Considering the MDCT unit, the number of detector rows is an important factor for a high-quality reconstruction: according to our review, a 64-detectors row is an appropriate device, and is currently a common one in forensic and medical imaging departments.

Most of the methods for virtual anthropology use submillimetric slice thickness. Based on her review, Uldin proposed a 0.625 mm slice thickness [7], however, this setting results in a time-consuming reconstruction that can slow down the entire process of victim identification. Moreover, this parameter is proposed in only 2 publications of our review on FHRs virtual re-association.

Images of millimetric slice thickness are quicker to acquire, and their association with a small spacing allows for precise reconstruction. It is used by 8 papers (3, 39, 40, 44, 50, 52, 62, 66) for FHRs reconstruction among the 15 providing their MDCT parameters. An alternative parameter would be to use thicker slices (1.25 mm) with a small interval (0.8 mm).

Both parameters (0.625mm and 1.25 mm) should be tested with the following protocol for fragmented remains reconstruction in order to obtain the right balance between speed and precision of the acquisition phase.

Considering the surface scan acquisition, it has to be separately performed for each fragment, on a cleaned bone. In our opinion, it is too time-consuming, and therefore not appropriate for a DVI context, that necessits a quick acquisition of numerous fragments.

4.2. Segmentation of the MDCT-data in order to generate discrete closed surfaces:

From a qualitative point of view, the segmentation step is the bottleneck of the entire protocol. It should be fully automated and as precise as possible. Manual segmentation of numerous fragments is time-consuming, and can be excluded for the identification of mass disaster victims. Automatic simple thresholding can lead to over or under-segmentation of the fragments, especially in case of touching fragments that cannot be automatically distinguished.

Automatic multi-level thresholding provides better quality for fragment segmentation, but requires a preliminary triage of the fragments that visually distinguishes flat, short and long bones, and epiphysis from diaphysis. The region growing method provides more automated steps, but once more, cannot separate the fragments in contact with each other. An operator intervention is therefore needed. For this reason, the placing seeds method seems to be the most appropriate approach, considering its perspectives of automatic segmentation and touching fragments labeling and splitting.

4.3. Post-processing and surface generation:

In order to optimize the time of surface mesh reconstruction, many softwares can be used. Some licenses provide modules for both segmentation, conversion in surface mesh or point cloud format, and 3D treatment (e.g. Materialise®, Amira®, Geomagic®). Switching from one module to the other represents a gain of time, but the license itself may be expensive.

Home-built software may allow the same operations (e.g. Fragmento®, Physiguide®, or VIRTOPS®) and its application for forensic purposes would be interesting.

Freewares for segmentation (e.g. Fiji®, ITK-Snap®, Sliceviewer®) and for 3D modeling (e.g. Blender®, Cloudcompare®, GomInspect®, Meshlab®) seems to be the best choice for a DVI application, as they are charge-free and easily available to every forensic unit. While the segmentation options may be limited, many of these softwares benefit from continuous collaborative research and development program.

4.4. Identification of intact surfaces and fracture surfaces (optional step, depending of the chosen re-association method):

The identification of fracture surfaces needs to be quick and reliable. Operator-directed methods for fracture selection (slice by slice or onto the 3D model) can be very time-consuming. CT-intensity thresholding methods are quicker, but result in an underestimation of the fracture surfaces (these methods consider the exposed surface of trabecular bone as a fracture surface). The thresholding technique implies a previous calibration of the MDCT-scan, though in DVI context, the imaging devices might differ in type and parameters for each mission. Additionally, the bone density shows an inter-individual variation.

Roughness-based methods seem to be more suitable: roughness analysis of intact surfaces distinguishes fractured and intact surfaces by comparison with roughness values of intact bones (46). This method has the advantage of being fully automated, however, it requires a large database of intact bone models. Finally, the edge curvature and roughness analysis methods seem to be promising approaches for identifying sharp fracture edges. Moreover, the roughness method can also be used for further steps of the protocol later on.

4.5. Identification of matching fragments:

Operator-directed matching and first points in contact methods are too time-consuming in cases of high degree of fragmentation and commingling.

The surface-in-contact method is quicker (1 to 9 seconds per comparison) but while it is of interest to medical purpose, it would remain too time-consuming when dealing with thousands of multi-surfaces comparison.

Methods using surface extrapolation are quick, but would be difficult to implement onto small fragments, and flat or serial bones.

Roughness analysis of intact surfaces [67] has the advantage of identifying the bone element of the fragment. However, it has to be compared to a sex and population specific template, whereas in a DVI context, the sex and origin of the victims are frequently unknown. Thus, this method requires the previous setting of a 3D model database with homogenous ages and sex categorization. Although the method used by Mahfouz et al. (2017) seems to be currently inapplicable in a DVI context, it could be promising in the future.

Finally, the roughness analysis of fracture surfaces appears to be a rapid and easy method for pairwise matching. Based on clusters of features, this approach can also lead to a basic registration considering the complementary features as landmarks [31], [50].

None of the previously mentioned methods can be directly applied in a high fragmentation and numerous victims context. In order to restrain the potential matches, the use of different matrix - one for each bone type as planned for the segmentation step- can be considered. Each matrix contains “dormant” (possibly matching fragments) and “active sets” (reference fragments).

Thus, for the method applied by Huang et al. (2006) using fractured surface roughness analysis, a two-steps protocol is set up. First, fragments with the highest number of clusters, representing an active set of reference model, are reconstructed and merged (active sets): preliminary reconstruction by fragments merging would already eliminate important surfaces and therefore reduce the possibilities for placing small fragments. Secondly, the “small fragments” with fewer clusters are compared to the reconstructed one.

The choice of the fragments to re-associate can be validated, as in the article presented by Huang [31], by performing a constraint free registration (i.e. allowing interpenetration of the surfaces), using the roughness features as landmarks. Non-interpenetrating fragments would be considered as matching fragments.

While this roughness-based method is promising, it may still present limitations in a scenario of high fragmentation / numerous victims. Before the re-association protocol, some strategies must be applied to identify the best fragments as references (and later comparing them with the other fragments) and to reduce the number of fragments to be re-associated (e.g. applying a minimal size as exclusion factor). The choice of fragments to re-associate may be also weighted by an on-site distance factor. This would imply to register the precise position of every fragments during their recovery.

More studies are needed on this point unless advanced technologies (e.g. artificial intelligence and more specifically machine learning) may enhance the identification of matching clusters.

4.6. Registration of matching fragments:

The final registration of matching surfaces leads to the reconstruction of fragmented models. The operator-directed methods of reconstruction in a virtual environment offers more reliable results than physical reconstruction [24] but they are still far too time-consuming for a DVI situation. Considering the surface extrapolation method for registration, its application on flat and serial bones (vertebra, ribs, etc.) can be hazardous. As for the matching, the first-point-in-contact method for the fragments registration is time-consuming.

Finally, the roughness analysis can lead to a first registration by the use of features as landmarks, with a final ICP method. This fine registration technique is used with most of the semi-automatic and automatic methods. The influence of the reference and moving surface choice would however to be investigated.

4.7. Validation of the re-association:

Mesh-to-mesh distance with the intact bone, or to intact statistical template (preferably to individual template) is an easy and validated method to evaluate if two fragments sufficiently fit to consider them as belonging to a single bone.

Most of the methods for fragments re-association are published as case reports without reproducibility studies. There is therefore a clear need for a validated protocols that can be applied in extreme situations (such as mass disaster missions) and brings a benefit when compared to manual pairwise matching and reconstruction. In consequence, intra-operator and inter-operator variability of the tested method should be evaluated, as well as the time needed for the complete protocol.

In the upcoming research, the percentage of reconstructed bone, the time needed and the sensibility/sensitivity of the chosen VRA methods constitute variables to consider and should be compared to physical methods, in order to evaluate the global operational efficiency of the built protocol.

Taphonomic processes, such as heat alteration, or plastic deformation of the bone may also represent crucial limits for the VRA method and their influence on its efficiency have to be evaluated [70]

5. CONCLUSION

In a DVI context, the virtual re-association of FHRs from the CT imaging would possibly make the identification process more efficient, by re-assembling the fragments from one individual before any physical examination and without any additional handling of the remains.

This review paper shows the state-of-the-art concerning different techniques for digitalizing fragmented bones and virtually re-assembling them. Approaches were tested in the field of forensic and paleoanthropology, but also from surgery planning, archaeology and morphometric geometrics. All of these specialties show an increasing interest for the virtual re-association of fragments:

Through the review of the considered published works and the evaluation of the applicability of the referenced methods for a DVI context, the following protocol for virtual re-association of FHRs is proposed:

1) Acquisition of the radiological image through the MDCT-scan, with a 64 detector rows device, and a slice thickness of 0.625mm / spacing 0.3mm or 1.25 / 0.8mm
2) Segmentation of the CT-data in order to generate discrete closed surfaces through the placing seeds methods
3) Post-processing and surface generation, using freewares allowing roughness analysis
4) Identification of intact surfaces and fracture surfaces by roughness analysis (optional step)
5) Identification of matching surfaces by roughness analysis
6) Registration of matching fragments, using roughness features as landmarks and refined by ICP
7) Validation of the registration by mesh-to-mesh comparison with the formerly scanned intact bone

Before being practically integrated to current guidelines, this protocol would have to be fully evaluated for its inter- and intra-operator variability, for sensibility/sensitivity, and for possible limitations due to heat alteration, plastic deformation of the bones, and size and number of the FHRs. Some methodological aspects such as the choice of the reference surface for the registration, and the perspective of a distance-weighted identification of matching fragments still need to be investigated.

The use of more advanced techniques, such as machine learning for the identification of fracture surfaces and for the matching step would considerably enhance the efficiency of the process.

Finally, this protocol of virtual re-association of FHRs may provide more extensive applications, not only for forensic purposes, but also in the archaeological and surgical fields.

Acknowledgments

We would like to thank Alejandro Dominguez, Christine Bruguier, André Guerra, Ruben Soto, radiographers at the University Center of Legal Medicine Lausanne-Geneva for supplying technical help. We are very grateful for the help of Stella Fahrni, specialist in forensic 3D documentation at the University Center of Legal

Medicine Lausanne-Geneva, for all technical advises. Furthermore, we thank Dr Claudine Abegg, forensic anthropologist at the Unit of Forensic Imaging and Anthropology, University Centre of Legal Medicine Lausanne-Geneva, for English editing.

REFERENCES:

[1] F. Gelaude, T. Clijmans, P. L. Broos, B. Lauwers, and J. Vander Sloten, “Computer-aided planning of reconstructive surgery of the innominate bone: Automated correction proposals,” *Comput. Aided Surg.*, vol. 12, no. 5, pp. 286–294, Jan. 2007, doi: 10.3109/10929080701684762.

[2] J. J. Jiménez-Delgado, F. Paulano-Godino, R. PulidoRam-Ramírez, and J. R. Jiménez-Pérez, “Computer assisted preoperative planning of bone fracture reduction: Simulation techniques and new trends,” *Med. Image Anal.*, vol. 30, pp. 30–45, May 2016, doi: 10.1016/j.media.2015.12.005.

[3] G.-Y. Wang, W.-J. Huang, Q. Song, Y.-T. Qin, and J.-F. Liang, “Computer-assisted virtual preoperative planning in orthopedic surgery for acetabular fractures based on actual computed tomography data,” *Comput. Assist. Surg.*, vol. 21, no. 1, pp. 160–165, Jan. 2016, doi: 10.1080/24699322.2016.1240235.

[4] M. Boudissa, H. Oliveri, M. Chabanas, and J. Tonetti, “Computer-assisted surgery in acetabular fractures: Virtual reduction of acetabular fracture using the first patient-specific biomechanical model simulator,” *Orthop. Traumatol. Surg. Res.*, vol. 104, no. 3, pp. 359–362, May 2018, doi: 10.1016/j.otsr.2018.01.007.

[5] S. Grabherr *et al.*, “Estimation of sex and age of ‘virtual skeletons’–a feasibility study,” *Eur. Radiol.*, vol. 19, no. 2, pp. 419–429, Feb. 2009, doi: 10.1007/s00330-008-1155-y.

[6] D. P. Sarment and A. M. Christensen, “The use of cone beam computed tomography in forensic radiology,” *J. Forensic Radiol. Imaging*, vol. 2, no. 4, pp. 173–181, Oct. 2014, doi: 10.1016/j.jofri.2014.09.002.

[7] T. Uldin, “Virtual anthropology : the forensic approach,” University of Geneva, 2016. doi: 10.13097/archive-ouverte/unige:94270.

[8] C. Abegg, I. Balbo, A. Dominguez, S. Grabherr, L. Campana, and N. Moghaddam, “Virtual anthropology: a preliminary test of macroscopic observation *versus* 3D surface scans and computed tomography (CT) scans,” *Forensic Sci. Res.*, pp. 1–8, Oct. 2020, doi: 10.1080/20961790.2020.1817270.

[9] S. Fahrni *et al.*, “CT-scan vs. 3D surface scanning of a skull: first considerations regarding reproducibility issues,” *Forensic Sci. Res.*, vol. 2, no. 2, pp. 93–99, 2017, doi: 10.1080/20961790.2017.1334353.

[10] H. Jung *et al.*, “Quantitative Analysis of Three-dimensional Rendered Imaging of the Human Skull Acquired from Multi-Detector Row Computed Tomography,” *J. Digit. Imaging*, vol. 15, no. 4, pp. 232–239, Dec. 2002, doi: 10.1007/s10278-002-0031-6.

[11] F. Dedouit *et al.*, “Virtual anthropology and forensic identification using multidetector CT,” *Br. J. Radiol.*, vol. 87, no. 1036, p. 20130468, Apr. 2014, doi: 10.1259/bjr.20130468.

[12] C. N. Stephan, S. S. D’Alonzo, E. K. Wilson, P. Guyomarc’h, G. E. Berg, and J. E. Byrd, “Skeletal Identification by Radiographic Comparison of the Cervicothoracic Region on Chest Radiographs a , b,” in *New Perspectives in Forensic Human Skeletal Identification*, Elsevier, 2018, pp. 277–292. doi: 10.1016/B978-0-12-805429-1.00024-7.

[13] S. Grabherr, C. Egger, R. Vilarino, L. Campana, M. Jotterand, and F. Dedouit, “Modern post-mortem imaging: an update on recent developments,” *Forensic Sci. Res.*, vol. 2, no. 2, pp. 52–64, Apr. 2017, doi: 10.1080/20961790.2017.1330738.

[14] Z. Obertová *et al.*, “Postmortem imaging of perimortem skeletal trauma,” *Forensic Sci. Int.*, vol. 302, p. 109921, Sep. 2019, doi: 10.1016/j.forsciint.2019.109921.

[15] A. Z. Mundorff, “Anthropologist-Directed Triage: Three Distinct Mass Fatality Events Involving Fragmentation of Human Remains,” in *Recovery, Analysis, and Identification of Commingled Human Remains*, B. J. Adams and J. E. Byrd, Eds. Totowa, NJ: Humana Press, 2008, pp. 123–144. doi: 10.1007/978-1-59745-316-5_7.

[16] H. H. de Boer, S. Blau, T. Delabarde, and L. Hackman, “The role of forensic anthropology in disaster victim identification (DVI): recent developments and future prospects,” *Forensic Sci. Res.*, vol. 4, no. 4, pp. 303–315, Oct. 2019, doi: 10.1080/20961790.2018.1480460.

[17] INTERPOL, “INTERPOL Disaster Victim Identification Guide.” 2018. [Online]. Available: https://www.interpol.int/How-we-work/Forensics/Disaster-Victim-Identification-DVI

[18] International Comittee of the Red Cross, “Gestion des dépouilles mortelles lors de catastrophes - Manuel pratique à l’usage des premiers intervenants - Deuxième édition.” 2018. [Online]. Available: ttps://shop.icrc.org/gestion-des-depouilles-mortelles-lors-de-catastrophes-manuel-pratique-a-l-usage-des-premiers-intervenants-669.html

[19] G. Grévin, P. Bailet, G. Quatrehomme, and A. Ollier, “Anatomical reconstruction of fragments of burned human bones: a necessary means for forensic identification,” *Forensic Sci. Int.*, vol. 96, no. 2–3, pp. 129–134, Sep. 1998, doi: 10.1016/s0379-0738(98)00115-7.

[20] D. W. Steadman, L. L. DiAntonio, J. J. Wilson, K. E. Sheridan, and S. P. Tammariello, “The Effects of Chemical and Heat Maceration Techniques on the Recovery of Nuclear and Mitochondrial DNA from Bone*,” *J. Forensic Sci.*, vol. 51, no. 1, pp. 11–17, Jan. 2006, doi: 10.1111/j.1556-4029.2005.00001.x.

[21] G. W. Weber, “Virtual Anthropology,” *Am. J. Phys. Anthropol.*, vol. 156, no. S59, pp. 22–42, 2015, doi: 10.1002/ajpa.22658.

[22] G. Jani, A. Johnson, and W. Belcher, “Case report: Digital restoration of fragmented non-human skull,” *Forensic Sci. Int. Rep.*, vol. 2, p. 100070, Dec. 2020, doi: 10.1016/j.fsir.2020.100070.

[23] A. L. Brough, B. Morgan, and G. N. Rutty, “Postmortem computed tomography (PMCT) and disaster victim identification,” *Radiol. Med. (Torino)*, vol. 120, no. 9, pp. 866–873, Sep. 2015, doi: 10.1007/s11547-015-0556-7.

[24] P. Urbanová, A. H. Ross, M. Jurda, and I. Šplíchalová, “The virtual approach to the assessment of skeletal injuries in human skeletal remains of forensic importance,” *J. Forensic Leg. Med.*, vol. 49, pp. 59–75, Jul. 2017, doi: 10.1016/j.jflm.2017.05.015.

[25] M. Jurda, P. Urbanová, and J. Chmelík, “Digital restoration of fragmentary human skeletal remains: Testing the feasibility of virtual reality,” *J. Forensic Leg. Med.*, vol. 66, pp. 50–57, Aug. 2019, doi: 10.1016/j.jflm.2019.06.005.

[26] S. Naji, C. de Becdeliévre, S. Djouad, H. Duday, A. André, and S. Rottier, “Recovery Methods for Cremated Commingled Remains,” in *Commingled Human Remains*, Elsevier, 2014, pp. 33–56. doi: 10.1016/B978-0-12-405889-7.00003-4.

[27] H. Tuller and U. Hofmeister, “Chapter 2 - Spatial Analysis of Mass Grave Mapping Data to Assist in the Reassociation of Disarticulated and Commingled Human Remains,” in *Commingled Human Remains*, San Diego: Academic Press, 2014, pp. 7–32.

[28] D. H. Ubelaker, “Contributions of forensic anthropology to positive scientific identification: a critical Review: Forensic Sciences Research: Vol 4, No 1,” *Forensic Science Research*, 2019. https://www.tandfonline.com/doi/full/10.1080/20961790.2018.1523704 (accessed Aug. 04, 2019).

[29] H. H. de Boer, J. Roberts, T. Delabarde, A. Z. Mundorff, and S. Blau, “Disaster victim identification operations with fragmented, burnt, or commingled remains: experience-based recommendations,” *Forensic Sci. Res.*, vol. 0, no. 0, pp. 1–11, May 2020, doi: 10.1080/20961790.2020.1751385.

[30] L. W. de Jong *et al.*, “Experience with postmortem computed tomography in the forensic analysis of the November 2015 Paris attacks,” *Forensic Sci. Res.*, vol. 5, no. 3, pp. 242–247, Jul. 2020, doi: 10.1080/20961790.2020.1802686.

[31] Q.-X. Huang, S. Flöry, N. Gelfand, M. Hofer, and H. Pottmann, “Reassembling fractured objects by geometric matching,” in *ACM SIGGRAPH 2006 Papers on - SIGGRAPH ’06*, Boston, Massachusetts, 2006, p. 569. doi: 10.1145/1179352.1141925.

[32] A. Willis, D. Anderson, T. Thomas, T. Brown, and J. L. Marsh, “3D reconstruction of highly fragmented bone fractures,” San Diego, CA, Mar. 2007, p. 65121P. doi: 10.1117/12.708683.

[33] U. Buck, S. Naether, M. Braun, and M. Thali, “Haptics in forensics: The possibilities and advantages in using the haptic device for reconstruction approaches in forensic science,” *Forensic Sci. Int.*, vol. 180, no. 2, pp. 86–92, Sep. 2008, doi: 10.1016/j.forsciint.2008.07.007.

[34] S. Winkelbach and F. M. Wahl, “Pairwise Matching of 3D Fragments Using Cluster Trees,” *Int. J. Comput. Vis.*, vol. 78, no. 1, pp. 1–13, Jun. 2008, doi: 10.1007/s11263-007-0121-5.

[35] S. Benazzi, E. Stansfield, C. Milani, and G. Gruppioni, “Geometric morphometric methods for three-dimensional virtual reconstruction of a fragmented cranium: the case of Angelo Poliziano,” *Int. J. Legal Med.*, vol. 123, no. 4, pp. 333–344, Jul. 2009, doi: 10.1007/s00414-009-0339-6.

[36] A. S. Chowdhury, S. M. Bhandarkar, R. W. Robinson, and J. C. Yu, “Virtual multi-fracture craniofacial reconstruction using computer vision and graph matching,” *Comput. Med. Imaging Graph.*, vol. 33, no. 5, pp. 333–342, Jul. 2009, doi: 10.1016/j.compmedimag.2009.01.006.

[37] B. Zhou, A. Willis, Y. Sui, D. Anderson, T. Thomas, and T. Brown, “Improving inter-fragmentary alignment for virtual 3D reconstruction of highly fragmented bone fractures,” Lake Buena Vista, FL, Feb. 2009, p. 725934. doi: 10.1117/12.810967.

[38] J. Fornaro, M. Keel, M. Harders, B. Marincek, G. Szekely, and T. Frauenfelder, “An interactive surgical planning tool for acetabular fractures: initial results,” *J. Orthop. Surg.*, vol. 5, p. 50, 2010, doi: 10.1186/1749-799X-5-50.

[39] S. Benazzi, F. L. Bookstein, D. S. Strait, and G. W. Weber, “A new OH5 reconstruction with an assessment of its uncertainty,” *J. Hum. Evol.*, vol. 61, no. 1, pp. 75–88, Jul. 2011, doi: 10.1016/j.jhevol.2011.02.005.

[40] S. Benazzi and S. Senck, “Comparing 3-Dimensional Virtual Methods for Reconstruction in Craniomaxillofacial Surgery,” *J. Oral Maxillofac. Surg.*, vol. 69, no. 4, pp. 1184–1194, Apr. 2011, doi: 10.1016/j.joms.2010.02.028.

[41] W. Yu, M. Li, and X. Li, “Fragmented Skull Modeling Using Heat Kernels,” p. 22.

[42] T. Kikuchi and N. Ogihara, “Computerized assembly of neurocranial fragments based on surface extrapolation,” *Anthropol. Sci.*, vol. 121, no. 2, pp. 115–122, 2013, doi: 10.1537/ase.130618.

[43] P. Olsson, F. Nysjo, J.-M. Hirsch, and I. B. Carlbom, “A haptics-assisted cranio-maxillofacial surgery planning system for restoring skeletal anatomy in complex trauma cases,” *Int. J. Comput. Assist. Radiol. Surg.*, vol. 8, no. 6, pp. 887–894, Nov. 2013, doi: 10.1007/s11548-013-0827-5.

[44] H. Amano *et al.*, “Virtual reconstruction of the Neanderthal Amud 1 cranium,” *Am. J. Phys. Anthropol.*, vol. 158, no. 2, pp. 185–197, Oct. 2015, doi: 10.1002/ajpa.22777.

[45] G. Du, M. Zhou, C. Yin, J. Zhang, Z. Wu, and W. Shui, “An automatic positioning algorithm for archaeological fragments,” in *Proceedings of the 15th ACM SIGGRAPH Conference on Virtual-Reality Continuum and Its Applications in Industry - Volume 1*, Zhuhai, China, Dec. 2016, pp. 431–439. doi: 10.1145/3013971.3013992.

[46] Irwansyah, J.-Y. Lai, T. Essomba, and P.-Y. Lee, “Algorithm for segmentation and reduction of fractured bones in computer-aided preoperative surgery,” in *Proceedings of the 3rd International Conference on Biomedical and Bioinformatics Engineering*, Taipei, Taiwan, Nov. 2016, pp. 12–18. doi: 10.1145/3022702.3022703.

[47] F. Di Vincenzo *et al.*, “Digital reconstruction of the Ceprano calvarium (Italy), and implications for its interpretation,” *Sci. Rep.*, vol. 7, no. 1, p. 13974, 25 2017, doi: 10.1038/s41598-017-14437-2.

[48] F. Paulano-Godino and J. J. Jiménez-Delgado, “Identification of fracture zones and its application in automatic bone fracture reduction,” *Comput. Methods Programs Biomed.*, vol. 141, pp. 93–104, Apr. 2017, doi: 10.1016/j.cmpb.2016.12.014.

[49] Irwansyah, N. P. Sinh, J. Y. Lai, T. Essomba, R. Asbar, and P. Y. Lee, “Integration of computer-assisted fracture reduction system and a hybrid 3-DOF-RPS mechanism for assisting the orthopedic surgery,” vol. 308, p. 012010, Feb. 2018, doi: 10.1088/1757-899X/308/1/012010.

[50] L. Vlachopoulos, G. Székely, C. Gerber, and P. Fürnstahl, “A scale-space curvature matching algorithm for the reconstruction of complex proximal humeral fractures,” *Med. Image Anal.*, vol. 43, pp. 142–156, Jan. 2018, doi: 10.1016/j.media.2017.10.006.

[51] C. Yin, M. Zhou, Y. Fan, and W. Shui, “Template-Guided 3D Fragment Reassembly Using GDS,” in *Image and Graphics Technologies and Applications*, Singapore, 2018, pp. 432–441. doi: 10.1007/978-981-13-1702-6_43.

[52] I. Irwansyah, J.-Y. Lai, and P.-Y. Lee, “Repositioning bone fragments using registration of paired-points and assisted constraints in virtual bone reduction surgery,” *Biomed. Eng. Appl. Basis Commun.*, May 2019, doi: 10.4015/S1016237219500212.

[53] S. Nguyen Phu, T. Essomba, I. Idram, and J.-Y. Lai, “Kinematic analysis and evaluation of a hybrid mechanism for computer assisted bone reduction surgery,” *Mech. Sci.*, vol. 10, no. 2, pp. 589–604, Dec. 2019, doi: https://doi.org/10.5194/ms-10-589-2019.

[54] A. Profico *et al.*, “Virtual Anthropology and its Application in Cultural Heritage Studies,” *Stud. Conserv.*, vol. 64, no. 6, pp. 323–336, Aug. 2019, doi: 10.1080/00393630.2018.1507705.

[55] A. J. Collings and K. Brown, “Reconstruction and physical fit analysis of fragmented skeletal remains using 3D imaging and printing,” *Forensic Sci. Int. Rep.*, p. 100114, Jun. 2020, doi: 10.1016/j.fsir.2020.100114.

[56] A. Johnson, G. Jani, J. A. Garriga, and A. Pandey, “Digital reconstruction of fragmented tooth remains in forensic context,” *Forensic Sci. Res.*, vol. 0, no. 0, pp. 1–6, Apr. 2020, doi: 10.1080/20961790.2020.1737462.

[57] G. Jani, A. Johnson, U. Parekh, T. Thompson, and A. Pandey, “Effective approaches to three-dimensional digital reconstruction of fragmented human skeletal remains using laser surface scanning,” *Forensic Sci. Int. Synergy*, vol. 2, pp. 215–223, Jan. 2020, doi: 10.1016/j.fsisyn.2020.07.002.

[58] N. A. Rasheed and J. Nordin, “A Survey of Computer Methods in Reconstruction of 3D Archaeological Pottery Objects,” *Int. J. Adv. Res.*, vol. 3, no. 3, p. 13, 2015.

[59] S. Lautenschlager, “Reconstructing the past: methods and techniques for the digital restoration of fossils,” *R. Soc. Open Sci.*, vol. 3, no. 10, p. 160342, Oct. 2016, doi: 10.1098/rsos.160342.

[60] D. Eslami, L. Di Angelo, P. Di Stefano, and C. Pane, “Review of computer-based methods for archaeological ceramic sherds reconstruction,” *Virtual Archaeol. Rev.*, vol. 11, no. 23, p. 34, Jul. 2020, doi: 10.4995/var.2020.13134.

[61] K. Rathnayaka, T. Sahama, M. A. Schuetz, and B. Schmutz, “Effects of CT image segmentation methods on the accuracy of long bone 3D reconstructions,” *Med. Eng. Phys.*, vol. 33, no. 2, pp. 226–233, Mar. 2011, doi: 10.1016/j.medengphy.2010.10.002.

[62] C. Y. Huang, P. Y. Lee, J. Y. Lai, L. J. Luo, Y. C. Tsai, and S. C. Lin, “Simultaneous Segmentation of Bone Regions Using Multiple-Level Threshold,” *Comput.-Aided Des. Appl.*, vol. 8, no. 2, pp. 269–288, Jan. 2011, doi: 10.3722/cadaps.2011.269-288.

[63] F. Paulano, J. J. Jiménez, and R. Pulido, “3D segmentation and labeling of fractured bone from CT images,” *Vis. Comput.*, vol. 30, no. 6, pp. 939–948, Jun. 2014, doi: 10.1007/s00371-014-0963-0.

[64] J. Nysjö, F. Malmberg, I.-M. Sintorn, and I. Nyström, “BoneSplit - a 3D texture painting tool for interactive bone separation in CT images,” 2015, Accessed: Jul. 12, 2020. [Online]. Available: http://dspace5.zcu.cz/handle/11025/17152

[65] D. D. Ruikar, K. C. Santosh, and R. S. Hegadi, “Automated Fractured Bone Segmentation and Labeling from CT Images,” *J. Med. Syst.*, vol. 43, no. 3, p. 60, Feb. 2019, doi: 10.1007/s10916-019-1176-x.

[66] Y. Zhang, R. Tong, D. Song, X. Yan, L. Lin, and J. Wu, “Joined fragment segmentation for fractured bones using GPU-accelerated shape-preserving erosion and dilation,” *Med. Biol. Eng. Comput.*, vol. 58, no. 1, pp. 155–170, Jan. 2020, doi: 10.1007/s11517-019-02074-y.

[67] M. R. Mahfouz, A. Mustafa, E. E. Abdel Fatah, N. P. Herrmann, and N. R. Langley, “Computerized reconstruction of fragmentary skeletal remains,” *Forensic Sci. Int.*, vol. 275, pp. 212–223, Jun. 2017, doi: 10.1016/j.forsciint.2017.03.017.

[68] A. Palamenghi, D. De Angelis, M. Cellina, C. Sforza, C. Cattaneo, and D. Gibelli, “Does the choice of the reference model affect the results of 3D-3D superimposition procedure? A comparison of different protocols for personal identification,” *Int. J. Legal Med.*, Mar. 2021, doi: 10.1007/s00414-021-02550-x.

[69] P. M. Flach *et al.*, “Imaging in forensic radiology: an illustrated guide for postmortem computed tomography technique and protocols,” *Forensic Sci. Med. Pathol.*, vol. 10, no. 4, pp. 583–606, Dec. 2014, doi: 10.1007/s12024-014-9555-6.

[70] C. O’Donnell, M. Iino, K. Mansharan, J. Leditscke, and N. Woodford, “Contribution of postmortem multidetector CT scanning to identification of the deceased in a mass disaster: Experience gained from the 2009 Victorian bushfires,” *Forensic Sci. Int.*, vol. 205, no. 1–3, pp. 15–28, Feb. 2011, doi: 10.1016/j.forsciint.2010.05.026.

FIGURES AND TABLES

Figure 1. Review methodology

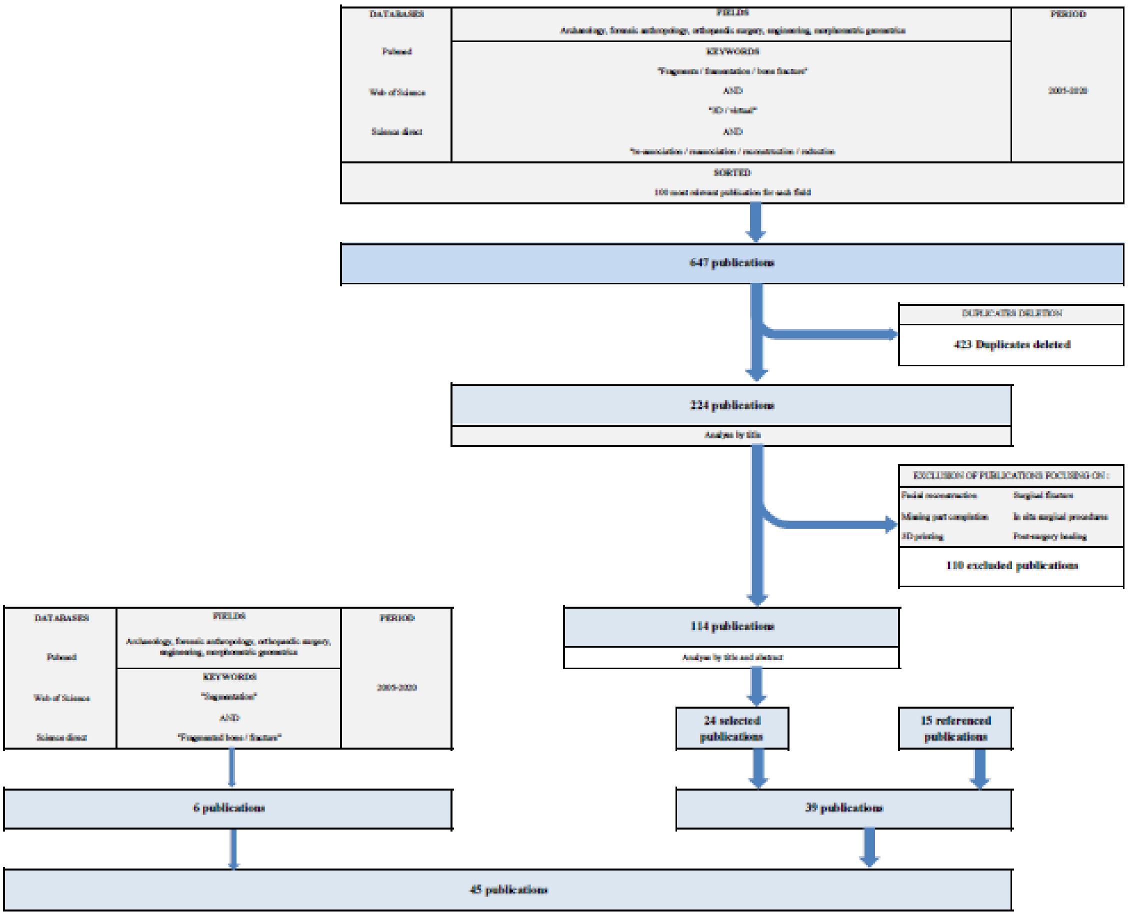

Figure 2. Quantitative evolution of fragments VRA publications from 2005 to 2020 (N=39)

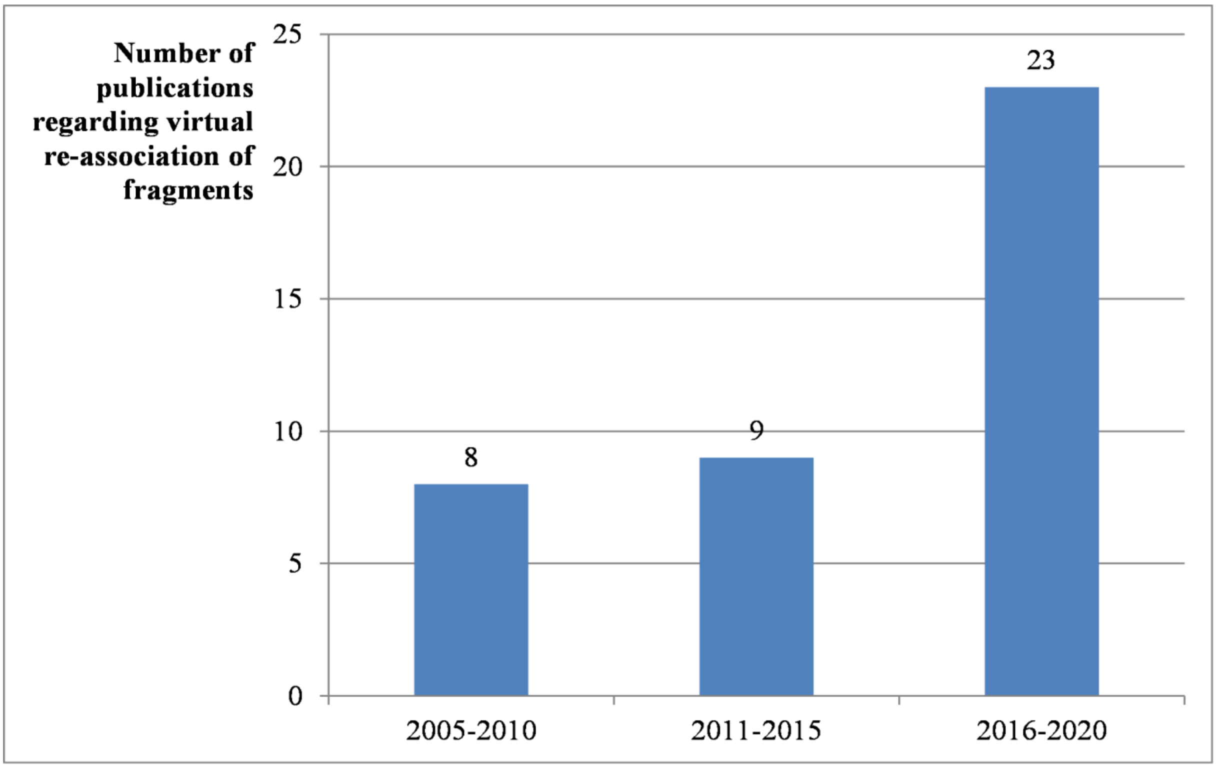

Figure 3. Fragments virtual re-association publications by scientific field (N=39). Some re-association protocols used both MDCT-scan and Surface scan

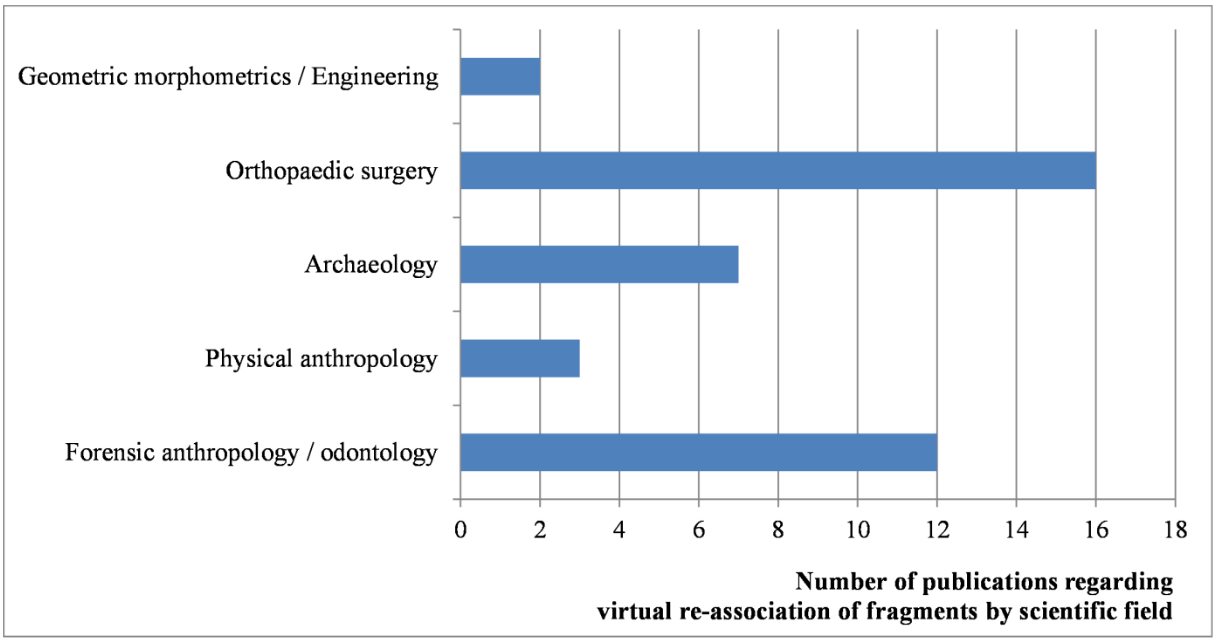

Figure 4. Data acquisition sources for fragments in the reviewed publications (N=39). Some re-association protocols used both MDCT-scan and Surface scan

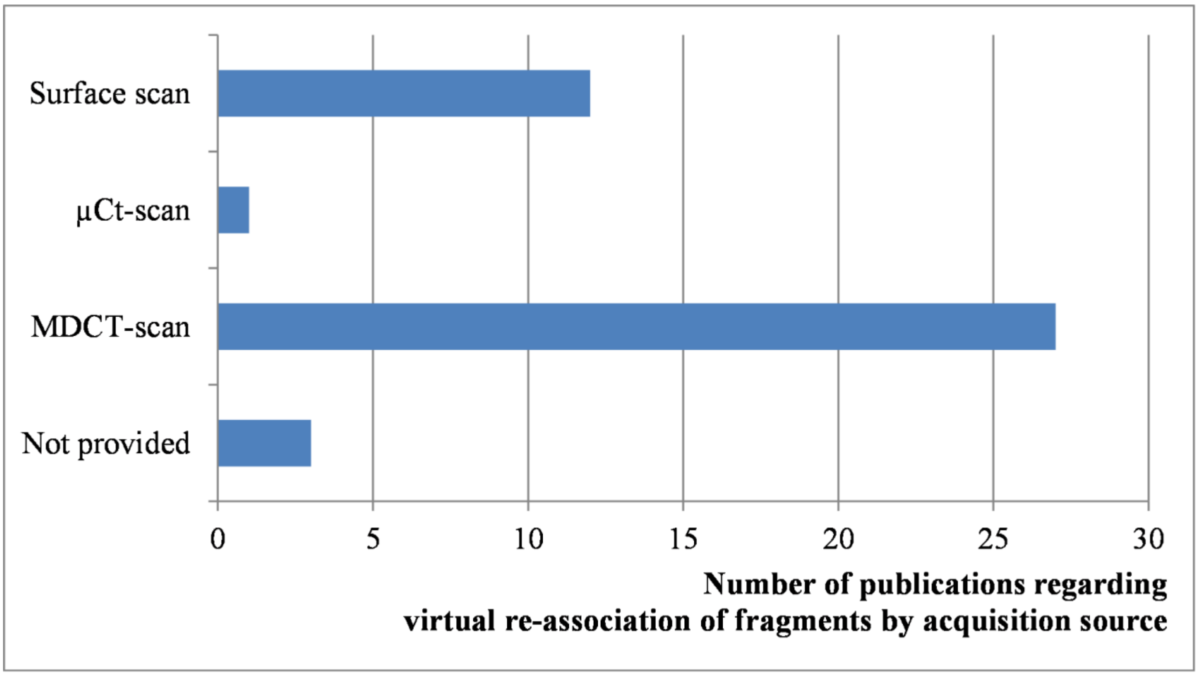

Figure 5. Segmentation methods for CT-scanned fragments in the reviewed publications (N=45). Some segmentation protocols require the association of different methods (e.g. thresholding and placing seeds or region growing techniques; multilevel thresholding and manual corrections)

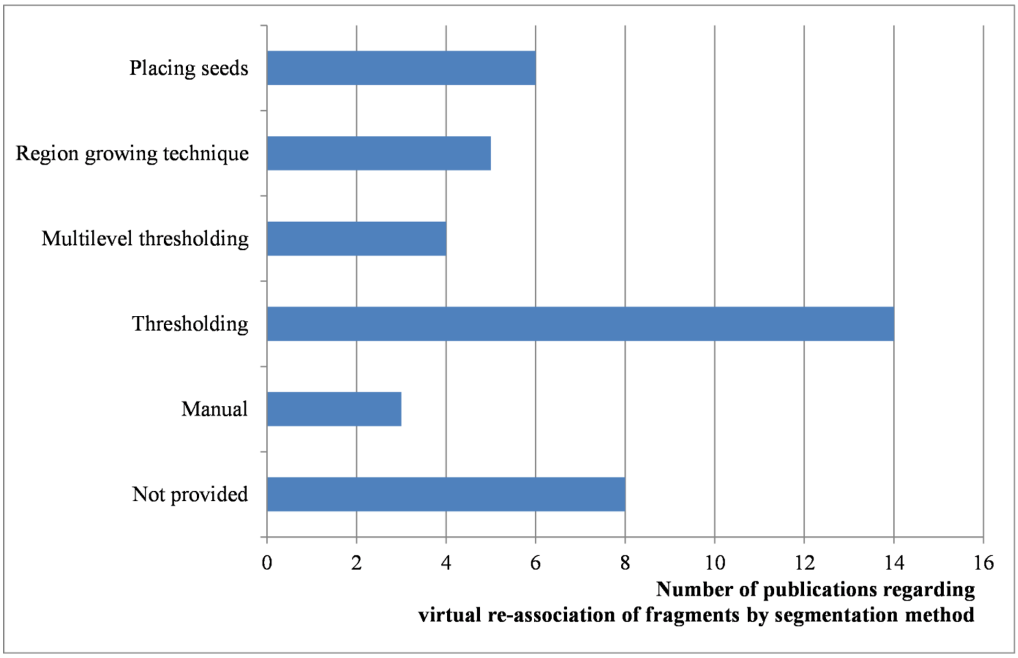

Table 1. Synthesis of the literature review

REVIEW OF FRAGMENTS VIRTUAL RE-ASSOCIATION IN FORENSIC ANTHROPOLOGY / FORENSIC ODONTOLOGY

PUBLICATION					SOURCE OF IMAGING		MATERIAL		SEGMENTATION TECHNIQUE		SURFACE MODELING		FRACTURED SURFACE IDENTIFICATION	MATCHING TECHNIQUE	FRAGMENTS REASSOCIATION		VALIDATION		
MAIN AUTHOR	REFERENCE	YEAR	PUBLICATION TYPE	FIELD	SOURCE	PARAMETERS	TYPE	NUMBER OF FRAGMENTS	FRAGMENT SEGMENTATION	SOFTWARE	TECHNIQUE	SOFTWARE		COMPLEMENTARY FRAGMENTS SELECTION	METHOD		ELEMENT OF COMPARISON	COMPARISON METHOD	
BUCK et al	33	2008	Primary	Forensic anthropology	MDCT scan + Surfac	MDCT-scan: / / Surface scan:	fractured long bones and skull	3	/	MDCT-scan: Slice vie	/	FreeForm Modeling Plus	/	Operator directed	Manual virtual reconstr	haptics	vs tool	TPS	color-coded poly

					escan	point spacing of 0.03 mm, the measuring noise amounts to 0.001 mm				wer / Slice viewer: /		(haptics)			uction				gonemesh
BENAZZI et al	35	2009	Primary	Forensic anthropology	MDCT-scan	64 detectors / slice thickness of 0.9 mm /	1 fragmented skull	/	Thresholding	Amira 4.0	Landmarks	PolyWorks 10.1 / Amira 4.0	/	Individual template	Individual template	Landmarks and semi-landmarks	Individual template	Landmarks	/

						increment 0.45 mm.													
DEDOUIT et al	11	2014	Review	Forensic anthropology	/	/	/	/	/	/	/	/	/	/	/	/	/	/	/
ULDIN	7	2016	Review (thesis)	Forensic anthropology	MD CT-scan	64 detector rows better than 8 detector rows/ 100 kV/ 12	Intact dry bones	/	Thresholding	/	/	Advantage Windows Server 2.0, GE Healt	/	/	/	/	/	/	/

						0 mA / 1 rot per sec / Slice thickness 0,625 mm / spacing 0,3 and 0,6 mm					h care							
MAHFOUZ et al	67	2017	Primary	Forensic anthropology	MDCT-scan + Surface	MDCT-scan: 0,625 x 0,625 x 0,	virtually fragmented in nominates,	fragmentation 10 to 30% / 2061 com	M / anual	Local shape variation (Gauss-	Fragmento	Roughness values	Location on statistical template + ICP (minimal roo	fine registration (ICP) / if th	location on statistical template +	statistical template	ICP + RMS + percentage	color-coded polygo

					scan	625 mm resolution	10 fragmented crania, innominates, humeri, femurs, 2061 commingled fragments	mingled fragments			Bonnet scheme method) + surface roughness			t squared error)	e residual registration error is smaller than FMS = rigorous identification	ICP (minimal root squared error)		of reconstrucion	nemesh
URBANOVA et al	24	2017	Primary	Forensic anth	Surfaces	high definitione	skull 17 fragmen	2 to 17	NA	Scan Studio	Desktop preco	Amira 5.0	/	operator directed	physical (3D		/	mesh distan	(Fidenti

				ropology	can	utral target scanning options, with 16 divisions/360/17k points/inch	ts / skull 2 parts / skull 2 fragments + vertebra, tibia, fibula foot fragments			HD 1.3.2 / post processing GOM Inspect software v.7.5 SRI	nstruction				printed replica) vs virtual (manual)			ce (ICP+RMS	s Analyst v1.32) intere-methinteroperator evaluation
JURDA, URBANOVA, CHM	25	2019	Primary	Forensic anthropol	MDCT-scan	full-body matrix: 1024 ×	3 virtually fragmente	03 to 14	Manual	Amira v5.0 + Ble	Desktop reconstruc	Cloud compare	/	Operator-directed	VR vs desktop rec	manual (aided by VR	Intact skull	Mesh distance (I	inter-method and

ELIK				ogy		1024 px/ slice thickness: 0.33 mm	d skulls			nder 2.78c	tion	2.9.1			onstruction	and desktop)		CP and RMS) with sound skull	inter-operator evaluation (Fidentis Analyst v1.32)
OBERTOVA et al	14	2020	Review	Forensic anthropolog	MDCT-SCAN, MR	/	/	/	/	/	/	/	/	/	/	/	/	/	/

				y	I, Surface scan														
JANI, JOHNSON, BELCHER	22	2020	Primary	Forensic anthropology	Surface scan	3D laser scanner FARO Edge 0.034 mm at Jet3D Scan	Fragmented dog skull	/	NA	/	Triangular mesh	Geomagic Studio 13	/	Operator directed	Manual	3 manually selected points registration	/	reconstructed printed model vs individual template	Landmarks, dimensions compared
JANI et al	57	2020	Primary	Forensic anthro	Surface sc	3D laser scanner	fragmented hum	7	NA	/	Triangular mes	Geomagic St	/	Operator directed	Manual	3 manually sele	/	reconstructe	Landmark

				pology	an		an mandible				h	udio 13				cted points registration		d printed model vs individual template	s, dimensions comparison
COLLINGS, BROWN	55	2020	Primary	Forensic anthropology	Micro-CT scan + Surface scan	slice thickness 0,025 mm / 80 kV / 7 W	1 fragmented archaeological human femur	2	Thresholding	Fiji, Amira	Triangular mesh	Amira, Geomagic Design X (2016)	/	operator directed on printed model (Physical fit analysis)	physical on printed model	/	operator directed: visual assessment, air space	/	/

JOHNSON et al	56	2020	Primary	Forensic odontology	Surface scan	accuracy 0,040µm	10 intact teeth (incisors)	4-May	NA	/	Triangular mesh	Geomagic Studio	/	operator directed	multipoint registration onto the fracture line + ICP	mesh-to-mesh comparison / measurement	mesh-to-mesh distance

REVIEW OF FRAGMENTS VIRTUAL RE-ASSOCIATION IN PHYSICAL ANTHROPOLOGY

PUBLICATION					**SOURCE OF IMAGING**		**MATERIAL**		**SEGMENTATION TECHNIQUE**		**SURFACE MODELING**		**FRACTURED SURFACE IDEN**	**MATCHING TECHNIQUE**	**FRAGMENTS REASSOCIATION**	**VALIDATION**	
MAIN AUTH	SENIO	**YEAR**	**PUBLIC**	**FIELD**	**SOURC**	**PARAM**	**TYPE**	**NUMBE**	**FRAGM**	**SOFTW**	**TECHN**	**SOFTW**		**COMPLEM**	**METHOD**	**ELEME**	**COMPARISON METHOD**

OR	RAUTHOR		**ATIONTYPE**		**E**	**ETERS**		**ROFFRAGMENTS**	**ENTSEGMENTATION**	**ARE**	**IQUE**	**ARE**	**TIFICATION**	**ENTARYFRAGMENTSSELECTION**			**NTOFCOMPARISON**		
KIKUCHI, OGIHARA	42	2013	Primary	Physical Anthropology	MDCT-scan	/	Virtually fragmented fossil (neurocrania)	5	/	/	/	/	/	Operator directed	Surface extrapolation	/	Intact skull	Mesh-to-mesh distance	+ automatic vs operator-directed re-association

PROFICO et al	54	2019	Primary	Physical Anthropology	MDCT-scan	/	Virtually fragmented bone	/	/	/	/	/	/	Operator directed	LM template GPA	RDIGITAL ALIGNMENT TOOL	Intact skull	RMS	/
BENAZZI et al	39	2011	Primary	Physical anthropology	MDCT-scan	Slice thickness 1 mm.	Fragmented fossil skull		Manual	Amira 5.2	Polyworks 10.1	/	/	Operator directed	Individual template + symmetry	LM and SLM	/	/	/

REVIEW OF FRAGMENTS VIRTUAL RE-ASSOCIATION IN FORENSIC ARCHAEOLOGY

PUBLICATION	**SOURCE OF IMAGING**	**MATERIAL**	**SEGMENTATION TECHNIQU**	**SURFACE MODELING**	**FRACTU**	**MATCHING**	**FRAGMENTS REASSOCI**	**VALIDATION**

									E				RED SURFACE IDENTIFICATION	TECHNIQUE	ATION		
MAIN AUTHOR	SENIOR AUTHOR	YEAR	PUBLICATION TYPE	FIELD	SOURCE	PARAMETERS	TYPE	NUMBER OF FRAGMENTS	FRAGMENT SEGMENTATION	SOFTWARE	TECHNIQUE	SOFTWARE		COMPLEMENTARY FRAGMENTS SELECTION	METHOD	ELEMENT OF COMPARISON	COMPARISON METHOD
YIN et al	51	2018	Primary	Archaeology / Geometric morphometrics	Surface Scan	/	Fragmented objects		NA	/	Triangular mesh	/	Local shape	Template-guided (geodesik disk spectrum) = roughness / curvature	ICP /	Mesh-to-mesh comparison	Mesh-to-mesh distance (ratio to total distan /

												ce of bounding box)
HUANG et al	31	2006	Primary	Archaeology / Paleo-Anthropology	Surface scan /	Fragmented objects 6 to 30	NA /	Point cloud /	Roughness analysis (algorithm automatically segments the fragments into a set of faces bounded by sha	Roughness analysis (features clusters) / simultaneous registration of corresponding fragments + elimination of	Multipieces local constrained registration then refined ICP /	Visual assessment / /

														rp curves)	interpenetrating matching					
RASHEED, NORDIN	58	2015	Review	Archaeology/ engeneering	/	/	/		/	/	/	/	/	/	/	/	/	/	/
AMANO et al	44	2015	Primary	Archeology/ PaleoAnthropology	MDCT-scan	120 kV, 200 mA, and 1 mm / Cross-sectional images were	1 fragmented deformed skull fossil	6	Thresholding + region growing techniques + Manual corrections	Avizo 6.1	Triangular mesh	Analyze 9.0	/	Automatic by surface extrapolation	Semi-auto	Bezier curves (intact surface extrapolation)	Individual template	TPS	Mesh distance

						reconstructed at 1 mm intervals, with a pixel size of 0.375 mm.													
DU et al	45	2016	Primary	Archaeology/Paleo-Anthropology	Surface scan	/	Fragmented object	120 fragments	NA	/	Triangular mesh	/	/	Template-guided (geodesik disk spectrum)	ICP	/	Visual assessment	/	/

LAUTENSCHLAGER	59	2016	Review	PaleoAnthropology	/	/	/		/	/	/	/	/	/	/ /	/	/ /
ESLAMI et al	60	2020	Review	Archaeology/ engeneering	/	/	/		/	/	/	/	/	/	/ /	/	/ /

REVIEW OF FRAGMENTS VIRTUAL RE-ASSOCIATION IN FORENSIC ORTHOPEDIC SURGERY

PUBLICATION					**SOURCE OF IMAGING**		**MATERIAL**		**SEGMENTATION TECHNIQUE**		**SURFACE MODELING**		**FRACTURED SURFACE ID**	**MATCHING TECHNIQUE**	**FRAGMENTS REASSOCIATION**	**VALIDATION**	
MAIN	SEN	**YEA**	**PUB**	**FIE**	**SOU**	**PAR**	**TYP**	**NUM**	**FRA**	**SOF**	**TEC**	**SOF**		**COMPL**	**METHOD**	**ELE**	**COMPARISON**

AUTHOR	IORAUTHOR	**R**	**LICATIONTYPE**	**LD**	**RCE**	**AMETERS**	**E**	**BEROFFRAGMENTS**	**GMENTSEGMENTATION**	**TWARE**	**HNIQUE**	**TWARE**	**ENTIFICATION**	**EMENTARYFRAGMENTSSELECTION**			**MENTOFCOMPARISON**	**METHOD**	
WILLIS et al	32	2007	Primary	Orthopedic surgery	MDCT-scan	0.2 to 0.5mm/slice spacing of 0.3 or 0.5mm	Clinical CT-scans of fractured tibia	/	Thresholding	Matlab	/	/	Thresholding (statistical choice gaussian curves cortical and cancellaneous bone).	Operator-directed	ICP (matching surface geometry) + Weight Hounsfield du	/	/	/	/

															nit intensity				
ZHOU et al	37	2009	Primary	Orthopedic surgery	MDCT-scan	/	Fragmented bone surrogate (polymer) + radioopacification agent	/	Thresholding + contour extraction	/	/	/	Mesh --> fracture surface = trabecular	Operator-directed landmarks	Automated landmarks alignment + weight for patches on cortical area	ICP	/	/	/

CHOWDHURY et al	36	2009	Primary	Orthopedic surgery	MDCT-scan /	Fractured mandible /	Thresholding /	/ /	Operator-directed	Maximum Weight Graph Matching algorithm: spatial proximity (Hausdorff distance) and mathematical formulation of surface caracteristics (contour cur	ICP through matching points determined by MWGM and MSE /	Individual template	Maximum Cardinality Minimum Weight bipartite graph matching algorithm /

														vature)					
FORNARO et al	38	2010	Primary	Orthopedic surgery	MDCT-scan	/	7 fractured coxal bones	/	/	Amira	/	OpenGL	/	Operator directed + haptics	/	/	/	/	/
BENAZZI, SENCK	40	2011	Primary	Orthopedic surgery	MDCT-scan	Slice thickness 0,625 to 1 mm	Intact skulls	/	Thresholding	Amira 5.2	/	Rapidform	Operator-directed	Operator-directed	Landmarks + TPS with intact skull	/	Intact skull	RMS	/
OLSSON et al	43	2013	Primary	Orthopedic surgery	MDCT-scan	Slice thickness 0,35 mm/sp	Fragmented skull	8	Thresholding + manual correctio	Matlab + ITK-SN	/	Nvidia Quadro 40	/	Operator directed + haptics	Operator directed +	/	Visual assessment	/	/

						acing 0,65 mm			ns	AP		00 Graphics Processing Unit			haptics				
WANG et al	3	2016	Primary	Orthopedic surgery	MDCT-scan	Slice thickness 1.5 mm	13 patients with pelvic and acetabular fractures	/	Thresholding + manual corrections	/	/	VIRTOPS + Mimics	/	Operator-directed	Manual virtual	/	/	Healing criterion	/
IRWANSIAH et al	46	2016	Primary	Orthopedic surgery	MDCT-scan	/	fragmented bones	/	Multilevel thresholding + Placing	Physiguide	Point cloud	Physiguide	/	Operator-directed	Landmarks (operator	/	Visual assessment	/	/

									seeds (automatic seeds selection)						-directed features on fracture line) + ICP				
JIMENEZ-DELGADO et al	2	2016	Review	Orthopedic surgery	MDCT-scan	/	/	/	/	/	/	/	/	/	/	/	/	/	/
VLACHOPOULOS et al	50	2017	Primary	Orthopedic surgery	MDCT-scan	Resolution 512*512 0,625 mm sp	Fragmented tibia + fibula / talus /	5 fragments (tibia + fibula)	Thresholding + Placing seeds (2D)	/	Point cloud	/	OBB sweeping and gridding for contact	Highest number of contact points (after repeati	ICP	/	/	ICP + RMS + percentag	/

						acing	calcaneus						points between 2 surfaces + refined by distance analysis then curvature analysis	ng segmentation of fracture surface for each potential pair)				e of reconstrucion	
BOUDISSA et al	4	2018	Primary	Orthopedic surgery	MDCT-scan	/	14 acetabular fractures	/	Thresholding + region growing + manual corrections	ITK-SNAP	/	ArtiSynth + ITK-SNAP		Operator-directed	Operator-directed	/	/	Healing criterion	/

VLACHOPOULOS et al	50	2018	Primary	Orthopedic surgery	MDCT-scan	slice thickness 1 mm / 120kV /	16 fractured proximal humerus (4 cadaveric simulated fracture)	2 to 5, mini 195 mm2	Thresholding + region growing + manual corrections	Matlab 2015	/	/	Curvature analysis	Fracture line 3D curvature analysis (complementarity of signed curvature in scale-space and best match when reduction is maximal)	Landmarks on the fracture line	RMS for distance between points of both surfaces	Visual assessment for clinical cases, RMS with intact model for cadaveric	RMS	/
IRWANSHYA et	49	2018	Primary	Orthopedi	MDCT-s	/	Fragmented	4	Multilevel thres	Physiguid	Point clou	Physiguid	/	Operator-directed	Landmar	/	Visual assess	/	/

al				c surgery	can		bones		holding + Placing seeds (automatic seeds selection)	e	d	e			ks (operator-directed features on fracture line) + ICP		ement		
IRWANSHYA, LAI, LEZ	52	2019	Primary	Orthopedic surgery	MDCT-scan	512x512 pix, slice thickness 1,5 mm	Fragmented bones	4	Multilevel thresholding + Placing seeds	physiguide	Triangular mesh	Physiguide	Operator-directed	Operator-directed	LM curvature analysis	Curve-to-curve correspondance	Intact bone	RMS	/

NGUYEN PHU et al	53	2019	Primary	Orthopedic surgery	MDCT-scan	/	Fragmented bones	2	/	Physiguide	/	/	/	Operator-directed	Operator-directed /	Visual assessement	/ /

REVIEW OF FRAGMENTS VIRTUAL RE-ASSOCIATION IN FORENSIC GEOMETRIC MORPHOMETRICS / ENGENEERING

PUBLICATION					**SOURCE OF IMAGING**		**MATERIAL**		**SEGMENTATION TECHNIQUE**		**SURFACE MODELING**		**FRACTURED SURFACE IDENTIFICATION**	**MATCHING TECHNIQUE**	**FRAGMENTS REASSOCIATION**	**VALIDATION**	
MAIN AUTHOR	SENIOR AUTHOR	**YEAR**	**PUBLICATION TYPE**	**FIELD**	**SOURCE**	**PARAMETERS**	**TYPE**	**NUMBER OF FRAGMENTS**	**FRAGMENT SEGMENTATION**	**SOFTWARE**	**TECHNIQUE**	**SOFTWARE**		**COMPLEMENTARY FRAGMENTS SELECTION**	**METHOD**	**ELEMENT OF COMPARISON**	**COMPARISON METHOD**

WINKELBACH, WAHL	34	2008	Primary	Geometric Morphometrics / Engeneering	MDCT-scan	/	Fractured femora	2	/	/	/	/	/	Normales alignement + cluster tree matching strategy	Multipieces local constrained registration	/	Angular deviation of matching results	/	/
YU, LI, LI	41	2012	Primary	Geometric Morphometrics / Engeneering	Surfaces scan	/	Digitally fragmented skulls	6	/	/	point cloud?	/	/	Local and gobal shape variation (heat kernel signature) + location on template	Automated coarse alignment on template +	/	Visual assessment	/	/

											refined by least square transformation error	

SHORT REVIEW OF BONE FRAGMENTS SEGMENTATION FROM MDCT IMAGING

PUBLICATION					**SOURCE OF IMAGING**		**MATERIAL**		**SEGMENTATION TECHNIQUE**		**SURFACE MODELING**		**FRACTURED SURFACE IDEN**
MAIN AUTHOR	SENIORAUT	**YEAR**	**PUBLICATION**	**FIELD**	**SOURCE**	**PARAMETER**	**TYPE**	**NUMBEROFF**	**FRAGMENTSE**	**SOFTWARE**	**TECHNIQUE**	**SOFTWARE**	

	HOR		**TYPE**			**S**		**RAGMENTS**	**GMENTATION**				**TIFICATION**
RATHNAYAKA et al	61	2011	Primary	Physical anthropology	MDCT-scan	64 rows detector / kVp = 140, in-plane pixel size = 0.39 mm × 0.39 mm and slice spac	5 ovin hindlimb	/	multilevel thresholding / Canny edge detection / Canny filter	Matlab for canny edge detection / Amira 5.1 for multilevel thresholdi	/	Amira 5.1	Canny edge detection and Canny filter --> better resolution than visual thresholding

						ing = 0.5 mm				ng			
HUANG et al	62	2011	Primary	Orthopedic surgery	MDCT-scan	Slice thickness 1.0-1.4 mm / Spacing 0.66-0.832 mm	Fragmented bones	/	Initial threshold T select all bone tissue + placing seeds (automatic placing seeds using increasing threshold)	/	/	/	/

PAULANO, JIMENEZ, PULIDO	63	2014	Primary	Orthopedic surgery	MDCT-scan	/	Fracture lower limb	/	Thresholding + placing seeds	/	Point cloud	/	thresholding + placing seeds (2D) +
NYSJÖ et al	64	2015	Primary	Orthopedic surgery	MDCT-scan	/	Fragmented skll	/	Placing seeds (on 3D reconstructed models)	Python	/	Python	/
RUIKAR, SANTOSH, HEGADI	65	2019	Primary	Orthopedic surgery	MDCT-scan	/	Fragmented bones	/	Slice by slice contrast enhancement algorithm (grey	Matlab?	/	/	/

									histogram) / mask / Region growing technique				
ZHANG et al	66	2020	Primary	Orthopedic surgery	MDCT-SCAN	Slice thickness 1,0 et 2,0 mm	Fragmented bones	/	GPU accelerated segmentation (normal based erosion + region growing + record-ba	/	/	/	/

							se dilation)	

Table 2. Softwares for segmentation and modeling of FHR surfaces

SOFTWARES	**REFERENCES**	
	SEGMENTATION	**3D MODELING**
Amira	*24, 25, 35, 38, 39, 40, 44, 61*	*24, 38, 44, 55, 61, 65*
ArtiSynth		*4*
Blender		*25*
Cloudcompare		*25*
Fiji	*55*	
Fragmento	*67*	*67*
Freeform Modeling		*33*
Geomagic		*2, 22, 55, 56, 57*
GomInspect		*24*
ITK-Snap	*4, 43*	
Landmarks		*2*
MatLab	*32, 43, 61*	*50*
Maya	*2*	
Meshlab		*2*
Materialise (Mimics and 3Matics)		*3*
Physiguide	*48, 49, 52, 53*	*52*
Polyworks		*40*
Rapidform XR		*40, 54*

ScanStudio		*24*
Spiers		*2*
Sliceviewer	*33*	
VGStudio		*2*
Virtops		*3*

Table 3. Descriptive processes for identifying the fracture surfaces

METHODS			**REFERENCES**
CT-INTENSITY BASED METHODS	THRESHOLDING		32, 37, 61
	PLACING SEEDS		63
	REGION GROWING		32.65
POST-SEGMENTATION METHODS	OPERATOR-DIRECTED METHODS		34, 36, 40, 52
	ROUGHNESS / CURVATURE ANALYSIS	Template	67
		Intrinseque roughness	31, 50
	FIRST POINT IN CONTACT METHODS		48

Table 4. Descriptive processes for pairwise matching of complementary fragments

METHODS			***REFERENCES***
OPERATOR-DIRECTED METHODS			3, 4, 22, 24, 25, 32, 33, 37, 38, 39, 40, 42, 43, 46, 47, 49, 52, 53, 56, 57
AUTOMATED METHODS	GLOBAL SHAPE	Fragment-to-fragment	*42, 44*
	VECTORIAL REGISTRATION / FIRST POINTS IN CONTACT		*34, 63*

	GEOMETRIC MORPHOMETRICS PUZZLE SOLVING		*36*
	ROUGHNESS / CURVATURE ANALYSIS	Template	*45, 51, 67*
		Fragment-to-fragment	*31, 41, 50, 52*

Table 5. Descriptive processes for the registration of matching fragments

METHODS			***REFERENCE***
OPERATOR-DIRECTED	PHYSICAL (printed model)		*56*
	VIRTUAL	Desktop environment	*3, 4, 22, 24, 53, 56,*
		Virtual reality	*25, 47*
		Haptics	*33, 38, 43*
SEMI-AUTOMATIC	GLOBAL SHAPE		*42, 44*
	ROUGHNESS / CURVATURE ANALYSIS		*31, 41, 67*
	LANDMARKS		*22, 36, 39, 40, 41, 48, 49, 50, 52, 54, 57, 56*
AUTOMATIC	VECTORIAL REGISTRATION / FIRST POINT IN CONTACT		*48, 64*
	FINE REGISTRATION (ICP / LSTE)		*2, 24, 32, 37, 45, 46, 51, 67*

AUTHORS CONTRIBUTION:

Lise MALFROY CAMINE: Conceptualization, Data curation, Formal analysis, Methodology, Writing- original draft, **Vincent VARLET:** Conceptualization, Supervision, Methodology, Project administration, Writing – review and editing, Visualization, Validation, **Lorenzo CAMPANA:** Resources, Formal analysis, Writing- review and editing **Silke GRABHERR:** Supervision, Project administration, Writing- review and editing, Validation, **Negahnaz MOGHADDAM:** Conceptualization, Supervision, Methodology, Project administration, Writing – review and editing, Validation.

DECLARATIONS OF INTEREST:

None

FUNDING SOURCES:

This research did not receive any specific grant from funding agencies in the public, commercial, or not-for-profit sectors.

HIGHLIGHTS:

- MDCT and physical re-association of fragmented human remains by forensic anthropologists are integrated in the DVI (Disaster Victims Identification) guidelines
- A protocol for virtual re-association of fragmented human remains (FHRs) would be highly beneficial in a DVI context
- Virtual methods for the re-association of fragmented bones or objects have been developed in the field of forensic anthropology, paleoanthropology, archaeology or medical planning of fractures reduction
- A critical review of existing methods for virtual re-association of fragmented bones or objects is performed
- Guidelines concerning FHRs re-association, using MDCT-imaging are provided for DVI protocol integration